

Recent Developments from ASACUSA on Antihydrogen Detection

B. Kolbinger^{1,*}, C. Amsler¹, H. Breuker², M. Diermaier¹, P. Dupré², M. Fleck¹, A. Gligorova¹, H. Higaki³, Y. Kanai⁴, T. Kobayashi⁵, M. Leali⁶, V. Mäckel¹, C. Malbrunot^{7,1}, V. Mascagna⁶, O. Massiczek¹, Y. Matsuda⁵, D.j. Murtagh¹, Y. Nagata⁸, C. Sauerzopf¹, M.C. Simon¹, M. Tajima⁴, S. Ulmer², N. Kuroda⁵, L. Venturelli⁶, E. Widmann¹, Y. Yamazaki², and J. Zmeskal¹

¹Stefan Meyer Institute for Subatomic Physics, Austrian Academy of Sciences, Boltzmannngasse 3, 1090 Vienna, Austria

²Ulmer Fundamental Symmetry Laboratory, RIKEN, Saitama 351-0198, Japan

³Graduate School of Advanced Science of Matter, Hiroshima University, Kagamiyama, Higashi-Hiroshima, 739-8530 Hiroshima, Japan

⁴Nishina Center for Accelerator-Based Science, RIKEN Saitama 351-0198, Japan

⁵Institute of Physics, University of Tokyo, 153-8902, Japan

⁶Dipartimento di Ingegneria dell'Informazione, Università degli Studi di Brescia, I-25133 Brescia, Italy and Istituto Nazionale di Fisica Nucleare, Sez. di Pavia, I-27100 Pavia, Italy

⁷CERN 1211, Geneva 23, Switzerland

⁸Department of Physics, Tokyo University of Science, Shinjuku, Tokyo 162-8601, Japan

Abstract. The ASACUSA Collaboration at CERNs Antiproton Decelerator aims to measure the ground state hyperfine splitting of antihydrogen with high precision to test the fundamental symmetry of CPT (combination of charge conjugation, parity transformation, and time reversal). For this purpose an antihydrogen detector has been developed. Its task is to count the arriving antihydrogen atoms and therefore distinguish background events (mainly cosmic) from antiproton annihilations originating from antihydrogen atoms which are produced only in small amounts. A central BGO crystal disk with position sensitive read-out detects the annihilation and a surrounding two-layered hodoscope is used for tracking charged secondaries. The hodoscope has been recently upgraded to allow precise vertex reconstruction. A machine learning analysis based on measured antiproton annihilations and cosmic rays has been developed to identify antihydrogen events.

1 Introduction

According to current cosmological theory, matter and antimatter have been created in equal parts after the Big Bang. However, the observed matter-antimatter asymmetry in the universe today cannot be explained quantitatively by the Standard Model of particle physics.

Potential clues could be found by the precise investigation of the spectrum of the antihydrogen atom (\bar{H}) and comparison with its matter counterpart which is known to high precision [1–3]. In this

*e-mail: bernadette.kolbinger@oeaw.ac.at

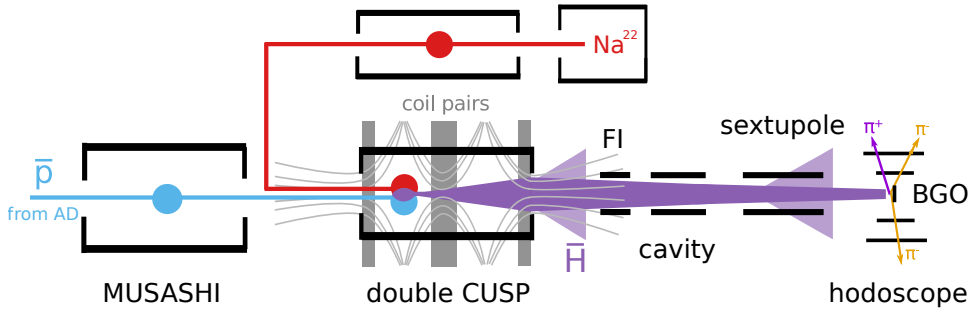


Figure 1. Sketch of the ASACUSA-CUSP setup. Antiprotons are drawn in blue, positrons in red. The produced antihydrogen atoms and the polarising effect of the double CUSP field and the sextupole magnet are indicated in purple (dark purple for low field seekers and light purple for high field seekers).

context, the ASACUSA collaboration at the Antiproton Decelerator (AD) of CERN aims to test the CPT symmetry by measuring the ground state hyperfine splitting of antihydrogen. The CPT theorem states that any local, Lorentz invariant quantum field theory should conserve CPT. From that theorem ensues that atoms and antiatoms should have the same atomic spectra.

ASACUSA is performing a Rabi-like experiment to measure the hyperfine transitions of \bar{H} in a beam [4]. A sketch of the beamline is displayed in Figure 1. For the production of \bar{H} , antiprotons (\bar{p}) extracted from the AD are further decelerated by a radio frequency quadrupole before being stored in a Penning-Malmberg type catching trap, named MUSASHI [5]. The positrons from a ^{22}Na source are accumulated in another Penning trap, before being transported to the mixing trap [6], the so-called double CUSP trap [7]. The latter is composed of multi-ring electrodes providing a static electric field, and two pairs of anti-Helmholtz coils. In the presence of a magnetic field, the ground state of (anti)hydrogen exhibits four hyperfine states which can be classified into high- and low-field seekers, according to their behaviour in an inhomogeneous magnetic field. The \bar{H} atoms formed in the mixing process leave the double CUSP trap as a polarised beam due to the magnetic field gradient of the trap which focuses low-field seekers and defocuses atoms in high-field seeking states.

The \bar{H} atoms enter the spectroscopy beam line located directly downstream of the mixing trap. It consists of a microwave cavity for inducing transitions between high and low field seeking states, and a superconducting sextupole magnet for state selection [4, 8]. The spectroscopy apparatus has been tested with hydrogen [9]. The antiatoms are detected by a crystal calorimeter at the end of the beamline, surrounded by a segmented hodoscope made of plastic scintillators. As the amount of \bar{H} produced with the current techniques is low [10], a high detection efficiency for annihilations is needed. The antihydrogen detector and its recent upgrade will be discussed in the next section.

Since it is essential to know the amount of antihydrogen atoms exiting the production trap in the ground state, a field ioniser is placed directly after the mixing trap. Atoms above a certain principal quantum number n_{min} are ionised by the applied voltage ($n_{min} = 14$ at the highest field ioniser configuration used: $|\vec{E}| \approx 10 \text{ kV/cm}$). By recording the rate of antihydrogen events at the detector for different voltage settings, the quantum state distribution of the produced atoms has been measured for the first time [11]. The data-driven machine learning strategy used to achieve the results will be outlined briefly below.

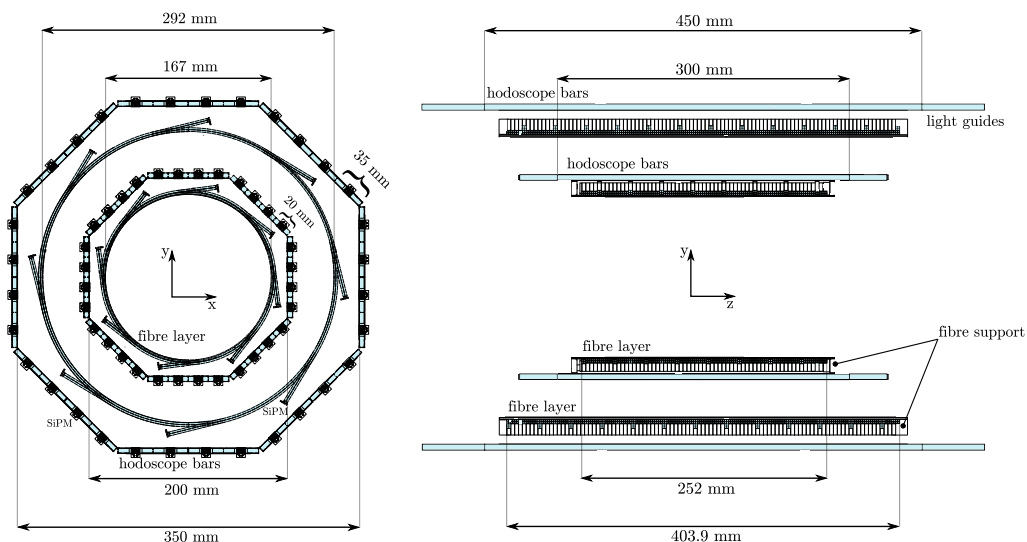


Figure 2. Drawing of the antihydrogen tracking detector. Top: cross section of the tracking detector perpendicular to the beam axis. The hodoscope bar layers and the two scintillating fibre layers are shown. Bottom: tracking detector in the y - z plane. Scintillators are coloured in light-blue, SiPMs in black.

2 The antihydrogen detector

The detector is composed of a central scintillating crystal target where the \bar{H} atoms annihilate, and a surrounding hodoscope for tracking the charged annihilation products (mainly pions).

The annihilating \bar{H} is detected with a 90 mm diameter bismuth germanate (BGO) disc with a thickness of 5 mm [12] coated with carbon on its upstream face. The crystal is placed in a vacuum vessel at UHV pressure. The BGO is read out by four Hamamatsu H8500C multianode photomultiplier tubes (MAPMT) with 8×8 channels, each connected to a Clearpulse CP80190 read-out unit. The MAPMT are separated from the BGO by a UHV viewport. The central detector is surrounded by the hodoscope detector, supported by a 1 mm thick stainless steel pipe.

A drawing of the two-layered, segmented hodoscope detector for tracking the charged annihilation products [13] is shown in Figure 2. The fibre upgrade discussed in section 4 is also shown. The hodoscope covers $\approx 80\%$ of the solid angle for annihilation products emitted from the centre of the BGO. Both layers are made of eight removable panels containing four 5 mm thick scintillating bars each. The outer layer has a diameter of 350 mm, the outer bars are 450 mm long and 35 mm wide. The diameter of the inner layer is 200 mm, its bars are 300 mm long and have a width of 20 mm. Light guides are attached on both sides of the bars to match the detecting area of the KETEK 3350TS silicon photomultipliers (SiPMs). Two SiPMs operated in series are glued to each light guide to increase the light collection. The SiPMs are read out using front-end electronics [14] and CAEN V1742 waveform digitisers.

The double sided readout of the scintillating bars reduces the dark noise by requiring of a coincidence between up and downstream SiPM. Also, it allows precise time measurement of the passing particles. Of particular interest is the resolution of the time difference between bars, which is a measure of the time of flight (ToF). The characterisation of the hodoscope detector was carried out with cosmic rays. The time of flight resolution between two opposing bars has been determined to be 552

± 5 ps (FWHM) for the outer layer and 497 ± 3 ps (FWHM) for the inner one [13]. Hence, the ToF is precise enough to discriminate between particles traversing the hodoscope from outside i.e. background and particles such as pions originating from the annihilation of antiprotons on the BGO.

Furthermore, from the time difference between signals recorded by the upstream and downstream SiPMs on the same bar, the hit position of the particle on the bar in beam direction can be obtained. The position resolution for outer bars was determined to be 73 ± 3 mm (FWHM) and 59 ± 4 mm (FWHM) for the inner hodoscope bars. Considering the length of the bars, the resolution is not good enough for precise vertex reconstruction and it is not possible to distinguish upstream annihilations in the direct vicinity of the BGO disc, resulting from high field seeking antihydrogen states or during antiproton extractions for annihilations studies. In section 4 the detector upgrade using scintillating fibres is discussed which enables tracking in three dimensions and precise vertex reconstruction to overcome these shortcomings. The upgrade will also improve the performance of the analysis described in the next section.

3 Analysis strategy

The analysis uses a supervised machine learning method with boosted gradient decision trees [15]. Measured data is used for training and validation of the algorithm. The signal data sample consists of measured antiproton annihilation events of antiprotons extracted from the MUSASHI to the antihydrogen detector [5]. This is possible since the event signature of antihydrogen and antiproton annihilation in the ASACUSA detector is the same. The background, which is dominated by cosmic particles, has been recorded during beam-off periods, with no antiproton delivery to ASACUSA. Therefore, the analysis will help to discriminate against cosmic background only. About 4000 antiproton and 30000 cosmic events are available for the machine learning procedure. 2/3 of the samples are used for training and 1/3 for testing. In order to overcome class imbalance and therefore avoid a biased algorithm, oversampling is used on the antiproton events of the training sample. An ensemble of algorithms each with a randomly selected training and validation set has been built. Detection efficiency and background rejection have been determined using the class predictions of the ensemble for the validation sets.

The achieved fraction of cosmics falsely identified as signal is under 0.25% and the detection efficiency for antiproton events is close to 80%. The algorithm can then be used to identify antihydrogen events during mixing runs. The first measurement of the quantum state distribution of antihydrogen atoms at the exit of the double cusp down to $n_{min} = 14$ as resulting from this analysis was recently published [11].

In total, 43 runs have been performed with the highest field configuration of the field ioniser. With this setting, atoms are ionised down to principal quantum number $n = 14$ and they are likely to decay to the ground state before reaching the cavity. The above described analysis identified about 0.16 events per run. In order to evaluate the significance, the p-value of the background-only hypothesis was computed using Poisson statistics. The p-value was then converted into units of σ (observed significance) via the unit gaussian. The found significance of the number of events with $n < 14$ is 4.5σ .

4 Hodoscope upgrade

The tracking detector has been upgraded in order to improve its position resolution in beam direction. The upgrade consists of two additional layers of scintillating fibres perpendicular to the existing hodoscope bars, see Figure 2. Each channel is made up of four 2×2 mm² square fibres. They are

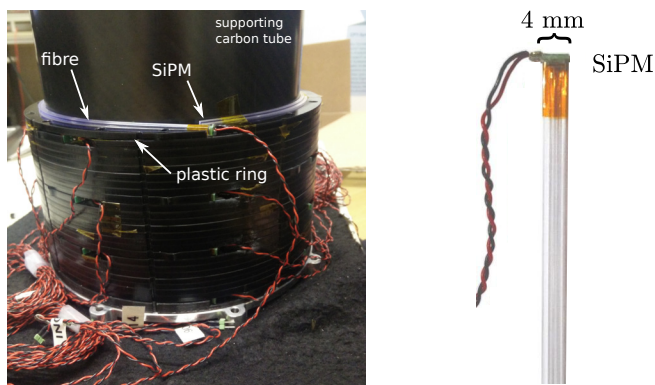


Figure 3. Left: assembly of the fibres on the carbon tube. Right: close up of a 4 mm×4 mm fibre bunch.

bundled together and glued to one SiPM (KETEK PM3350-EB) i.e. the read-out of the fibres is single sided. A close-up of one of the channels is shown in Figure 3 (right). The fibre bundles are wound once around the supporting carbon tube, covering one circumference with a small additional overlap to avoid loss of solid angle. They are kept in place by supporting plastic rings (indicated in Figure 2 and 3 (left)). The picture in Figure 3 (left) has been taken during the assembly of the detector.

The cladding of the fibres prevents cross talk which has been measured in the lab and was determined to be less than 1%. The inner layer houses 63 channels and has a diameter of 167 mm, whereas the outer one has 100 channels and a diameter of 292 mm. The front-end electronics powering and reading out the SiPMs is identical to that used on the scintillating bars, providing analogue and digital signal output. Two TDCs (CAEN V1190B with 64 channels, CAEN V1190A with 128 channels) are used to record the leading edge timestamp and the time over threshold of the signals.

The upgraded detector has been integrated into the experimental setup in 2017 and has been successfully used for antiproton annihilation studies. For these measurements, the BGO central detector setup has been replaced by a 2×2 array of Timepix3 [16] read-out chips bump-bonded to a 500 μm thick silicon sensor. It is capable of measuring pions and heavy nuclear fragments from the annihilation on a thin target foil in front of it.

The tracking and vertex reconstruction analysis is on-going. Figure 4 shows a cosmic event recorded with the upgraded tracking detector, where bars and fibres with a hit are indicated in colour.

On the right panel, the hodoscope bar and corresponding fibre hits are shown. The bar hodoscope hits are marked by crosses and are determined from the time difference of up- and downstream SiPMs, the width of the crosses are the 2σ errors. The squares show fibre channels with a hit highlighting both, the consistency of the two sub-detectors and the increased position resolution provided by the new fibre upgrade.

5 Summary

We have presented the ASACUSA antihydrogen detector which monitors the rate of arriving antihydrogen atoms at the end of the beam line. A data-driven analysis employing machine learning has been developed which was used to identify antihydrogen candidates during mixing runs for the measurement of the quantum state distribution. The rate of antihydrogen atoms is currently still too low to perform spectroscopy and reach the precision goal of ≈ 1 ppm. Therefore, the current focus lies on increasing the production rate and determining characteristics of the antiatoms.

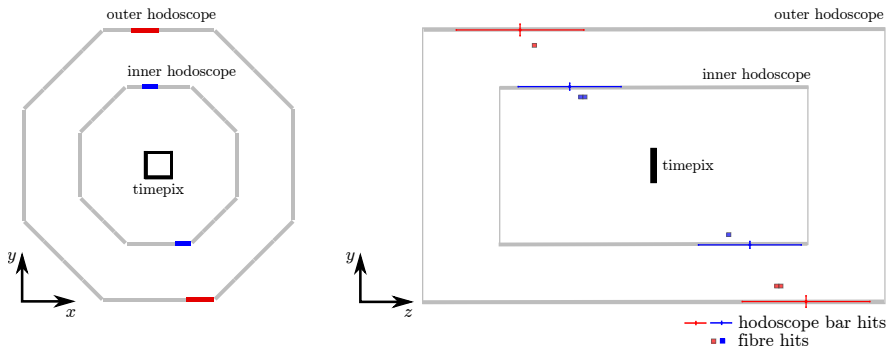


Figure 4. Cosmic event recorded during data taking in 2017. y-x plane (left) and y-z (right) plane of the detector are shown, where z is the direction of the beam. Bars and fibres with hits are indicated by crosses and squares respectively (blue for hits in the inner layers and red for the outer layers).

With the recent upgrade using scintillating fibres, the detector becomes capable of precise track and vertex reconstruction and therefore enabling the possibility to discriminate against additional background contributions such as annihilations close to the detector.

References

[1] Karschenboim S.G., Van. J. Phys. **78**, 639-678 (2000)
 [2] Parthey, C.G. et al., Phys. Rev. Lett. **107**, 203001 (2011)
 [3] Essen, L. et al., Nature **229**, 110-111 (1971)
 [4] Widmann, E. et al., Hyperfine Interactions **215**, 1-8 (2013)
 [5] Kuroda, N. et al., Phys. Rev. ST. Accel. Beams **15**, 024702 (2012)
 [6] Mohri, A. et al., Europhys. Lett. **63**, 207–213 (2003)
 [7] Nagata, Y. et al., Journal of Physics: Conference Series **635**, 022062 (2015)
 [8] Malbrunot, C. et al., Hyperfine Interactions **228**, 61-66 (2014)
 [9] Diermaier, M. et al., Nature Communications **8**, 15749 (2017)
 [10] Kuroda, N. et al., Nature Communications **5**, 3089 (2014)
 [11] Malbrunot, C. et al., Phil. Trans. R. Soc. A **376**, 20170273 (2018)
 [12] Nagata, Y. et al., Nuclear Instrum. Methods A **840**, 153-59 (2016)
 [13] Sauerzopf, C. et al., Nuclear Instrum. Methods A **845**, 579-582 (2016)
 [14] Sauerzopf, C. et al., Nuclear Instrum. Methods A **819**, 163-166 (2016)
 [15] Chen, T. et al., Xgboost: A scalable tree boosting system, ACM, proceedings of KDD'16 (2016)
 [16] Poikela, T. et al., Journal of Instrumentation **9** C05013 (2014)